Journal of Applied Polymer Science

# Orange Peel-Derived Pectin Jelly and Corn Starch-Based Biocomposite Film with Layered Silicates

**Zerrin Çokaygil,[1] Müfide Banar,[1] A. Tuğrul Seyhan[2]**
[1]Department of Environmental Engineering, Faculty of Engineering, Anadolu University, Eskişehir, Turkey
[2]Department of Materials Science and Engineering, Faculty of Engineering, Anadolu University, Eskişehir, Turkey
Correspondence to: M. Banar (E-mail: mbanar@anadolu.edu.tr)

**ABSTRACT:** Orange peel-derived pectin jelly/corn starch-based biocomposite films with and without layered silicates (LSs) were prepared using melt extrusion followed by film die casting. To enhance interfacial compatibility, corn starch and LSs were chemically modified. Regardless of chemical modification or LS weight content, different pectin jelly-to-starch weight ratios (63/37, 60/40, 57/43, and 54/46) were considered to formulate the ingredients of biocomposite films in light of Taguchi-based predictions. X-ray diffraction (XRD), fourier transform infrared spectroscopy (FTIR), differential scanning calorimetry (DSC), thermal gravimetric analysis (TGA), scanned electron microscopy (SEM) and transmission electron microscopy (TEM) were systematically used to characterize corn starch, LSs, and biocomposite films. Among all the films considered, pectin jelly/modified (15%) starch-based biocomposite film (54/46 w/w) containing 0.25 wt % of pristine LSs was found to be the most promising in terms of texture structure and mechanical integrity. Furthermore, creep recovery, hydrophobicity, and water vapor and oxygen gas transmission rates of the most promising biocomposite film were experimentally determined. Based on the findings obtained, the overall performance of the biocomposite film was evaluated and weighed against the overall performance of a low-density polyethylene film. © 2014 Wiley Periodicals, Inc. J. Appl. Polym. Sci. **2014**, *131*, 40654.

**KEYWORDS:** biopolymers and renewable polymers; composites; films; clay

Received 12 October 2013; accepted 27 February 2014
**DOI: 10.1002/app.40654**

## INTRODUCTION

The amount of fruit waste generated increases with the fruit juice beverage production rate. The huge amount of these fruit wastes leads to discarding problems. In Turkey, about 1,689,921 tons of orange were produced in every year. It means when squeezed, about 760,000 tons of waste orange peels are generated in the facilities.[1] These waste peels are either discharged to the landfill areas or end up being sent to the farms to be used as animal feeds. Deriving profitable byproducts from these fruit wastes has therefore become a recent matter of concern in the scientific community. Of all the likely byproducts derived from the fruit wastes, pectin is considered the most valuable. Waste orange peels hold therefore promise to be a great feedstock for sustainable pectin extraction. Mangiacapra et al.[2] reported that as pectin is water soluble and biodegradable, pectin extracted from waste orange peels is vital to developing environmentally friendly biodegradable materials. In addition to this, pectin forms edible films in pure form when blended with other polysaccharides such as starch.[3] Starch is a natural renewable polysaccharide and exists in the form of fine white granules composed of amylose and amylopectin accompanied by the basic composite unit of glucose. Starch has been cited as one of the most promising renewable source-based polymers owing to its large scale of availability and low cost.[4] However, especially following aging, starch-based polymers are sensitive to moisture and becomes brittle compared with typical synthetic polymers. Therefore, they are mostly considered a substitute candidate for a particular type of synthetic polymers for which a fast chemical decomposition is of concern. On the other hand, to accomplish commercially acceptable products, starch is usually blended with other polymeric materials able to improve its physical properties while minimizing its water sensitivity. However, in this case, proper adjustment of processing temperature and dwell time is certainly required to compensate for the rheological property differences between starch and the polymeric material of choice. To alleviate this problem, as another practical approach, starch is generally blended with low content of nanofiller constituents such as layered silicates (LSs). LSs with and without chemical modification are commonly used to develop functional polymer nanocomposites.[5] They are composed of a central alumina octahedral sheet sandwiched between two silica tetrahedral sheets. These nanofillers have hydrophilic characteristics owing to the presence of inorganic cations ($Na^+$ and $Ca^{2+}$) in the interlayer spacing.[6–13] They are thus miscible with various hydrophilic polymers including starch.[6–8]

There are a number of studies in the literature on starch-based biodegradable films in which pectin and LSs were either used as

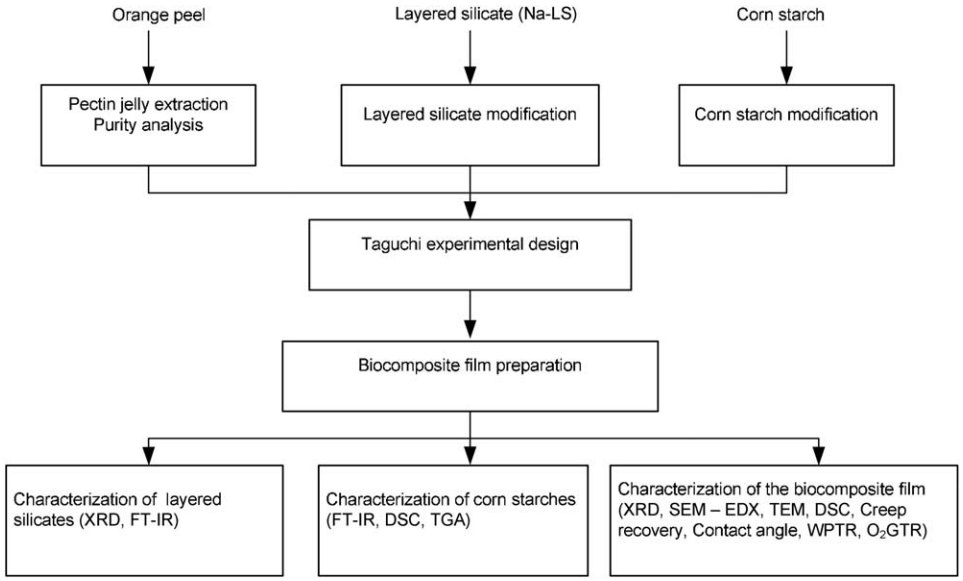


**Figure 1.** Flowchart of the study.

chemical stability provider or as a filler constituent. Park et al.[6] revealed that the dispersion of organically modified LSs in the thermoplastic starch matrix depends on degree of hydrophobicity of the LSs, which is a matter of polar interactions between the silicate layers and the thermoplastic starch. Coffin and Fishman[9,10] mixed pectin and LSs with thermoplastic starch by conducting solution casting and melt-film extrusion. They reported the improved barrier properties for pectin and LS-modified films compared with neat films. Fishman et al.[11] carried out similar experiments and found that pectin improves the film texture structure significantly. Mangiacapra et al.[2] used ball milling to blend the ingredients. Coffin and Fishman[10] added almond hull-extracted pectin in powder form to a mixture of starch and glycerol so as to prepare biodegradable films by solvent casting. The common point in all the studies mentioned above is that they utilized pectin in powder form obtained from waste materials.

In light of the relevant studies in the literature, the aim of this study is to extract pectin jelly from orange peels and to blend it with corn starch and LSs to prepare biocomposite films. To our best knowledge, for the first time in the literature, we have used extracted pectin in jelly form as a chemical stability enhancer in biocomposite films with LSs. To enhance the compatibility and wettability among starch, LS, and pectin, starch and LSs were chemically modified. Taguchi experimental design analysis was executed to optimize the melt extrusion-film process parameters. Creep recovery, hydrophobicity, water vapor transmission rate (WVTR), and oxygen gas transmission rate ($O_2$GTR) of the most promising biocomposite films were measured and its overall packaging performance was evaluated and discussed in comparison to the properties of a low-density polyethylene (LDPE) film.

## EXPERIMENTAL

### Materials

Bentonite clay based on 90% sodium LS (Na-LS) ($d_{90} < 37$ $\mu$m) was purchased from Eczacibasi Corp (Turkey). The cation exchange capacity of the Na-LS is 90–100 meq/100 g. A regular and commercially available corn starch was used in this study. Hexadecyltrimethylammonium chloride (HTAC) and propylene oxide were provided from Sigma Aldrich. Sodium trimetaphosphate (STMP) and sodium tripolyphosphate (STPP) were purchased from Merck.

### Pectin Jelly Extraction

Figure 1 shows the flow chart that summarizes the experimental steps followed in this study. First of all, oranges obtained from the local market were peeled. The peels obtained were then sliced into very small pieces with a thickness of ~0.5 cm. The slices were then sun dried and divided into two subgroups as albedo and flavedo. The procedure for pectin extraction from orange peels was reconsidered from the previous method.[12] It is to be noted that no precipitate occurred during extraction of flavedo with ethanol; thus, only extracts obtained from albedo were processed in this study. The purity of the prepared pectin jelly was examined, measuring its galacturonic acid content in accordance with the experimental procedure described by Ranganna.[14] The tests were repeated thrice and the purity of pectin jelly was found to be 65.37% ± 2.15%.

### Layered Silicate Modification

The organically modified LSs (O-LSs) were prepared according to the experimental procedure described by Tabtiang et al.[15] and Saka et al.[16] In brief, the Na-LS (20 g) was homogenously dispersed in deionized water (500 mL) at 80°C. Solutions of HTAC with different Na-LS contents (5, 15, 25, and 50%) were prepared with dissolution of 5 mL HCl in 100 mL deionized water. The final solution obtained was heated and stirred for 3 h. The filtration, while soaking, was repeated four or five times until a portion of the filtrate gave no opalescence with $AgNO_3$. The filtrate was allowed to dry at 55°C for 24 h, followed by milling and sieving on a screen of 125 $\mu$m.

### Corn Starch Modification

Corn starch was modified with propylene oxide in the presence of phosphate salts. The etherification reaction took place at

**Table I.** Selected Factors and Their Respective Levels

| Factors | Symbol | Level 1 | Level 2 | Level 3 | Level 4 |
|---|---|---|---|---|---|
| Starch type | A | Native (N) | 5% Modified (5M) | 10% Modified (10M) | 15% Modified (15M) |
| Pectin jelly/starch ratio | B | 63/37 | 60/40 | 57/43 | 54/46 |
| Layered silicate (LS) type | C | Na-LS | 15% Modified (15% O-LS) | 25% Modified (25% O-LS) | 50% Modified (50% O-LS) |
| LS content (wt %) | D | 0 | 0.25 | 0.45 | 0.70 |

40°C ± 2°C in 24 h, after propylene oxide (5, 10, and 15% v/w of starch solid) was subject to 40% starch slurry (pH 10.5) containing 15% sodium sulfate (dsb) and 5% sodium hydroxide. Following etherification, the modified starch was crosslinked for 2 h using 2% STMP and 5% STPP at 40°C ± 2°C, respectively. The pH of the starch slurry was then adjusted to 5.5 by using 10% of HCl aqua solution to terminate the reaction. The starch was filtered and the filter cake was washed with 5 vol of distilled water. The starch was dried at 40°C to attain final moisture content of 10–12%.

### Taguchi Experimental Design

The simple approach in research process involves changing one parameter at a time. Briefly, this approach requires that numerous experimental be tried to explore the entire parameter space. The experimental design approaches such as Taguchi method are considered an effective way to reduce the number of the experiments required for investigation of the effects of various parameters on the product quality and/or quantity. This method also screens the significant factors that are able to affect the response obtained from relatively insignificance factors, thus giving the optimum condition to attain the most desirable performance.[8]

In this study, Taguchi experimental design method was used to optimize the melt extrusion film process parameters. First, four main factors including starch type (A), starch content (B), LS type (C), and LS content (D) were considered in four levels (Table I). The factors and their levels have been selected based on some screening experiments. Use of a standard L16 orthogonal array, as shown in Table II, makes it possible to run 16 experiments instead of 256, based on a $4^4$ factorial experimental design method. Taguchi design of experiment module integrated into MINITAB 15 statistic software was utilized on the basis of four factors and four levels for each factor involved. Each row of the matrix represents one run at a specified condition. To avoid the systematic bias, the sequence in which the corresponding runs were carried out was randomized.

### Biocomposite Film Preparation

Orange peel-derived pectin jelly/corn starch-based biocomposite films with and without LSs (0, 0.25, 0.45, and 0.70 wt %) were prepared using melt extrusion followed by die casting. Regardless of any modifications or LS weight content, different pectin jelly-to-starch weight ratios (63/37, 60/40, 57/43, and 54/46 w/w) were considered when formulating the film ingredients. The glycerol and water were used for the purpose of plasticizing starch. The ratio of mixture of glycerol and water to starch (regardless of modification) remains fixed for all the film formulations. Regardless of modification, after mixing, the ingredients including pectin jelly, water, glycerol, starch, and LSs were left overnight in an oven at 70°C. Dried mixtures were then blended by a knife mill (Retch) at 4000 rpm in counter and clockwise counter directions for a short time. A lab-scale twin-screw compounder (15 mL, DSM Xplore) with a cast-film apparatus (DSM Xplore) attached was used to prepare the pectin-based biocomposite film (Figure 2). For each batch involved, about 18 g of mixtures was compounded at 120°C and 100 rpm for 2 min. It is to be noted that the extrudes obtained at the end of the first batch were once again fed to the microcompounder at the same temperature with an additional dwell time of 2 min. Films coming out of a slit die were cooled by means of a chilled twin rollers. The speed of the collecting roller (speed-controlled roller) was adjusted to 165 rpm, whereas the torque of the running roller (torque-controlled roller) was adjusted to 50 N. The area of the die opening was confined into 0.2 mm × 35 mm to make sure that the extruded films ended up with a thickness of 0.2 mm and a width of 30

**Table II.** Taguchi L16 ($4^4$) Orthogonal Array of Designed Experiments Based on the Coded Levels

| Randomized trials | Factors | | | |
|---|---|---|---|---|
| | A | B | C | D |
| 1 | 5M | 60/40 | Na-LS | 0.45 |
| 2 | 10M | 54/46 | 15% O-LS | 0.45 |
| 3 | 10M | 57/43 | Na-LS | 0.70 |
| 4 | 5M | 54/46 | 25% O-LS | 0 |
| 5 | N | 57/43 | 25% O-LS | 0.45 |
| 6 | 15M | 57/43 | 15% O-LS | 0 |
| 7 | N | 60/40 | 15% O-LS | 0.25 |
| 8 | 15M | 60/40 | 25% O-LS | 0.70 |
| 9 | 5M | 57/43 | 50% O-LS | 0.25 |
| 10 | 10M | 60/40 | 50% O-LS | 0 |
| 11 | 5M | 63/37 | 15% O-LS | 0.70 |
| 12 | 15M | 54/46 | Na-LS | 0.25 |
| 13 | N | 54/46 | 50% O-LS | 0.70 |
| 14 | 15M | 63/37 | 50% O-LS | 0.45 |
| 15 | N | 63/37 | Na-LS | 0 |
| 16 | 10M | 63/37 | 25% O-LS | 0.25 |

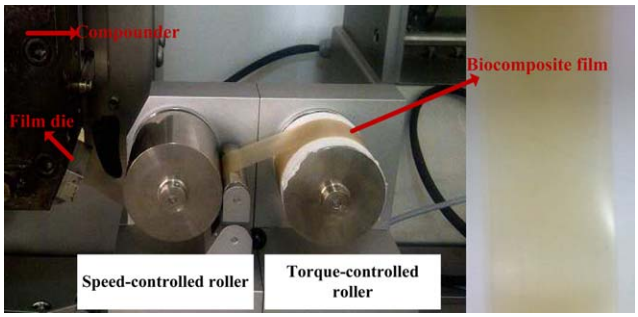


**Figure 2.** Co-rotating twin-screw laboratory-scale compounder and cast-film line. [Color figure can be viewed in the online issue, which is available at wileyonlinelibrary.com.]

mm. All biocomposite films were kept overnight in a controlled humid atmosphere to ensure their texture structure and mechanical integrity.

### Characterization of LSs

X-ray diffraction (XRD) and FTIR spectroscopy measurements were performed on the selected LSs with and without HTAC modification. XRD measurements were carried out conducting a Rigaku Rint 2000 diffractometer with CuK$\alpha$ radiation (XRD, $\lambda = 1$, 5406 Å, 40 kV, 40 mA). Samples were scanned at 1° $min^{-1}$ in the range of $2\theta = 2°$–10°. FTIR spectroscopy (Bruker-Tensor 27 FTIR) was also used in transmission mode to verify any functional group alterations that occur on LS surfaces following their chemical modification. For this purpose, the LSs with and without chemical modification are mixed with a very low content of KBr and pressed into thin-sheet pellets. The prepared pellets were eventually scanned from 500 to 4000 $cm^{-1}$ at a resolution of 4 $cm^{-1}$.

### Characterization of Corn Starches

FTIR, DSC, and TGA measurements were performed on the selected starch types with and without chemical modification just in the same manner as in the LS. More specifically, FTIR was used in transmission mode to verify any functional group alterations that occur in the starch structure following the chemical modification. For this purpose, once starch gels formed in ultrapure water (10% w/w) at 80°C, two drops of gels were sampled and subsequently cast onto $CaF_2$ window. All spectral outputs were recorded in the transmittance mode as a function of wave number in the range of 4000–400 $cm^{-1}$. Sixty-four scans were made for each spectrum with a 4 $cm^{-1}$ resolution. Thermal properties of starches were investigated using a TA Instruments DSC Q-2000 in regular mode. Starches (2.5 mg) were weighed on a balance and then placed in a 40-$\mu$L aluminum standard pan. Subsequently, 7.5 mg of ultrapure water was put in a pan using a microsyringe. After sealing, the pan was left stationary for 1 h to allow the sample in it to come to equilibrium. The sample was then scanned from 30 to 150°C with a heating rate of 10°C $min^{-1}$. At the end of each subsequent measurement, onset ($T_o$), intermediate ($T_p$), and completion ($T_c$) temperature values were recorded, so were the gelatinization enthalpy ($\Delta H$) values. Thermal degradation of starches was investigated using a TA Instruments TGA Q500. Samples of ~5–10 mg were placed in alumina precursors. The samples were then heated from room temperature to 600°C with a heating rate of 10°C $min^{-1}$ under nitrogen with a flow rate of 50 mL $min^{-1}$. The DSC and TGA results obtained were then evaluated in a concise manner.

### Characterization of the Biocomposite Film

Based on the Taguchi predictions, among 16 different types of the prepared biocomposite films, five survivals were considered to proceed the further experimental investigations. These corresponding biocomposite films were then stored at room temperature for 1 month to see the maintained elasticity. The most promising biocomposite film was selected based on the texture structure and mechanical integrity. The LDPE-based granules were used to produce a commercially used film to be cited as a reference for comparison purposes in some of the following characterization techniques.

Intrinsic viscosity of the most promising biocomposite film was measured by an Ubbelohde viscometer at 20°C, following the dissolution of the biopolymer in ultrapure water (0.1–0.5 g $dL^{-1}$). The molecular weight of the biocomposite film was calculated based on the intrinsic viscosity using Mark–Houwink equation as follows:

$$[\eta] = KM^a, \quad (1)$$

where $K$ and $a$ are the Mark–Houwink constants, $[\eta]$ is intrinsic viscosity, and $M$ is the molecular weight of the biopolymer.

A Rigaku Rint 2000 diffractometer with CuK$\alpha$ radiation (XRD, $\lambda = 1$, 5406 Å, 40 kV, 40 mA) was conducted to reveal the most promising biocomposite film structure. Biocomposite film was scanned at 1° $min^{-1}$ in the range of $2\theta = 2°$–60°. For comparison, a certain amount of Na-LS was also scanned at the same spectrum, keeping the experimental parameters unchanged.

SEM (SEM-Zeiss SUPRA 50 VP) attached with the backscattering (BE) detector at an acceleration voltage of 20 kV was used to visualize the dispersion state of the LS in the most promising biocomposite film. Before SEM examination, fracture surface of the biocomposite film was sputtered with gold–palladium coating to avoid overcharging. Energy-dispersive X-ray spectroscopy (EDX) analysis at an acceleration voltage of 20 kV was also performed.

Transmission electron microscopy (TEM) examination was carried out by using a FEI Tecnai G2 Spirit Bio (TWIN) electron microscope, operating at 80 kV, to visualize the dispersion state of the silicates within biocomposite film. The specimens were carefully cut at room temperature and placed onto 300-mesh carbon-coated grids by using an ultramicrotome. The overall morphological characteristics were then discussed in a concise manner.

The glass transition temperature measurements were performed using a TA Instruments DSC Q-2000 in a modulated mode (M-DSC). The most promising biocomposite film specimen was weighed in about 10 mg and heated from −20°C to 200°C at a rate of 3°C $min^{-1}$.

Creep recovery measurements were carried out to predict the packaging performance of the most promising biocomposite film. It helps predict whether or not polymer film of choice has

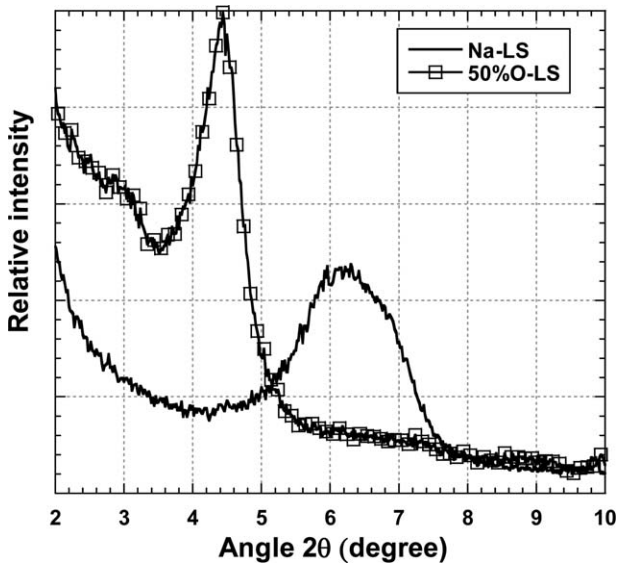


**Figure 3.** XRD patterns of Na-LS and 50% O-LS.

elasticity enough to recover its shape and stability. A measure of elasticity that can be obtained from a creep recovery experiment is the equilibrium recoverable compliance ($J_{er}$). In a regular creep recovery test, a stress is applied to the sample and the resultant strain generated at that stress level is measured for a specific time period. The stress is then dropped to zero and the recoverable strain is measured as a function of time. When all reversible deformation is recovered, the equilibrium recoverable compliance can be calculated as follows:

$$J_{er} = \frac{(\gamma_c - \gamma_r(t))}{\sigma}, \quad (2)$$

where $\gamma_c$ is the maximum strain in the creep zone, $\gamma_r(t)$ is the time-dependent recoverable strain, and $\sigma$ is the stress applied in the creep zone. The equilibrium recoverable compliance was calculated for each sample. The lower the equilibrium recoverable constant the sample shows, the higher the elasticity it has. In this study, creep recovery analyses were performed on films by using a dynamic mechanical analyzer, MetraVib DMA+450N. Some of the prepared composite films were preconditioned at 23°C and 50% relative humidity (RH) for 2 days before the creep recovery analysis was performed. A constant stress level of 0.75 MPa was applied to each film sample (10 min) of the same thickness and the resultant strain generated at that stress level was recorded for 20 min. The most promising biocomposite film was then compared to the LDPE film in terms of creep recovery performance.

To compare the water-resistant efficiency (hydrophobicity) between the most promising biocomposite film and a LDPE film, contact angles were measured using Biolin Scientific Attension contact angle instrument. Contact angles were measured by ultrapure water-based sessile drop method. Water surface tension was determined by the pendant drop method. The tabulated contact angle data were derived from average value of at least five measurements performed at room temperature in different points of the film surface.

WVTR (g $m^{-2}$ $h^{-1}$) of the most promising biocomposite and LDPE films was determined gravimetrically according to ASTM E96 standard method. The method is based on sealing a film to the open mouth of a test dish containing silica gel and placing the assembly into a controlled environmental chamber at 50% RH and 25°C. This allows for the required conditions with low humidity on one side of the film and high humidity on the other side. At least five film specimens were tested for each type of the films. The water vapor absorbed by silica gel was detected by weighing the test dish at different time intervals within 24 h. A linear regression was carried out to estimate the slope of this line in g $h^{-1}$.

$O_2$GTR of the films was also measured using an oxygen permeation instrument, Versaperm MK VI (Versaperm, England), according to ASTM F 1927 standard. Oxygen permeability of the most promising biocomposite and LDPE films was determined at constant temperature (23°C) and RH (50% RH). The films were placed between two sides of the test chamber. One side was exposed to carrier gas containing 100% $N_2$, whereas the other side was exposed to $O_2$ test gas with a purity of 99.97%. The sensor monitoring the exit port of the carrier gas side measured the amount of oxygen present. The measurement was completed when the concentration of oxygen in the exit of carrier gas was constant and then $O_2$GTR was calculated by using the following equation:

$$O_2\text{GTR} = \frac{E_s - E_0}{A}, \quad (3)$$

where $E_s$ and $E_0$ are "steady-state" and "zero" $O_2$GTR levels, respectively, and $A$ is the specimen area.

## RESULTS AND DISCUSSION

### Optimization of Biodegradable Composite Films

Neat and biocomposite films were produced by melt extrusion followed by die casting in the order as given in Table II. Based on the sample predictions obtained by Taguchi analysis, most of the composite films were successfully derived from the prepared blends. However, the films based on native starch with unmodified, 15 and 25% modified LSs were not able to be obtained as practically as expected. Regardless of modification, this was attributed to agglomeration of LSs in the native starch matrix. As a result, starch granules were not able to penetrate into silicate galleries. On the other hand, for the rigid and useful samples, platelets of the LSs under Van der Waals interactions were successfully separated from each other with the aid of the cationic modification. This is an indication of why only 50% O-LS was able to interact with native starch matrix in the way it is supposed to be. Moreover, when considering the rest of the produced films, LS modification was found to be almost inessential to produce composite films with modified starches. This is not only because starch modification by hydroxypropylation disrupts intermolecular and intramolecular hydrogen bonds and thus weakens the starch granular structure but also because the disrupted starch granules move into the LS galleries no matter how small their spacing is. From this point of view, starch modification by hydroxypropylation seems to help starch form useful films properly. It is to be noted that the studies under the following titles were carried out on the biocomposite films,

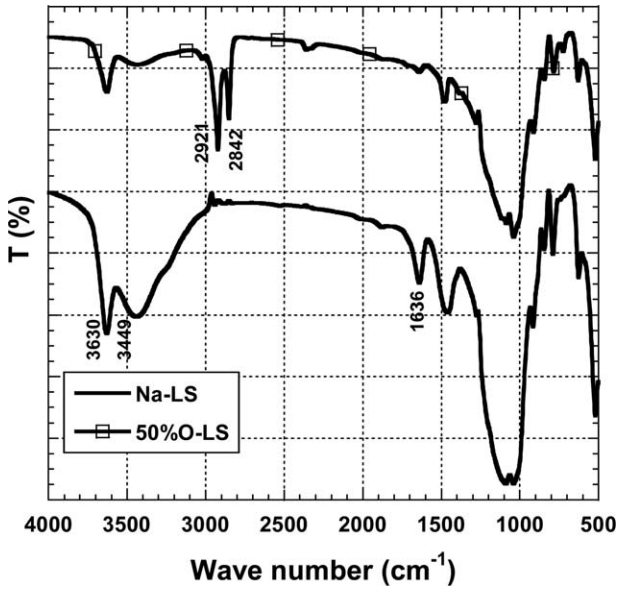


**Figure 4.** FTIR spectra of Na-LS and 50% O-LS.

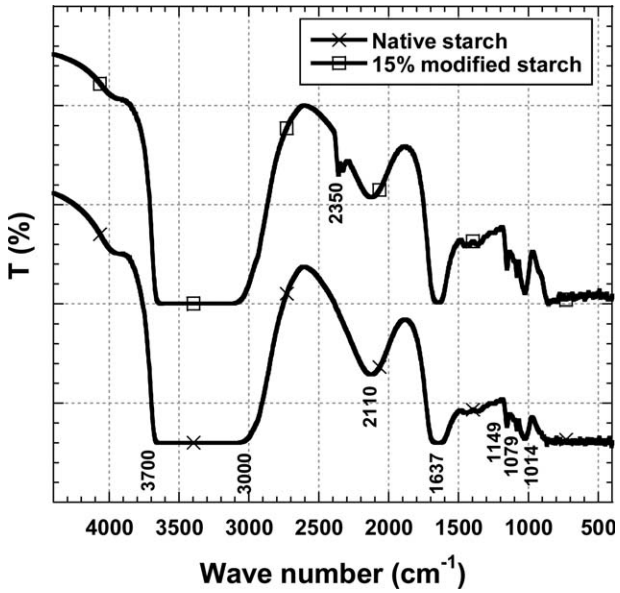


**Figure 5.** FTIR spectra of native and 15% modified starches.

with a particular emphasis on the predictions made by Taguchi analysis.

### Structure of the LSs

Figure 3 shows the XRD patterns for Na-LS and 50% O-LS. A characteristic diffraction peak with the 14.33 (Å) basal spacing appears at $2\theta = 6.16°$ for Na-LS. The value of $d_{(001)}$ for untreated Na-LS is supposed to be around 1.2 nm.

However, crystallite size and microstrain play an important role in final shape of the peak width and its intensity. As the LSs are obtained by ball milling in this study, mechanical shear and heat dissipation that manifest themselves as a microstraining may result in obtaining peak broadening. This makes it difficult to accurately interpret the peak point of the curve obtained, which may be the underlying reason for this interpretation. For 50% O-LS, the organic cation (ammonium ion) penetrates into the interlayer space of the LS and replaces the inorganic cation (sodium ion). As a result, it enlarges the gallery spacing (19.88 Å) and hence shifts the peak position toward a relatively low angle ($2\theta = 4.44°$), as depicted in the XRD pattern in Figure 3. This implies that the basal spacing is proportional to the size of cation or molecule between the layers. In other words, the sodium cation with the atomic radius of 1.02 Å and the ammonium ion with long-chain alkyl groups with a large radius of gyration resulted in the smallest and the greatest interlayer spacing in Na-LS and 50% O-LS, respectively. These findings are proportional to those obtained by Majdzadeh-Ardakani et al.[8]

Figure 4 shows the FTIR spectra of the Na-LS and 50% O-LS. The absorption bands at 3449 and 3630 $cm^{-1}$ that, respectively, correspond to —OH stretching and vibration of $H_2O$ within Na-LS become weaker than in 50% O-LS. In addition to this, the characteristic absorption bands of the symmetric and asymmetric stretching vibrations of the $—CH_2$ (2842 $cm^{-1}$) and of $—CH_3$ (2921 $cm^{-1}$) were observed on the IR spectra of 50% O-LS. In contrast to the IR spectra of Na-LS, the absorption band of —OH bending vibration of $H_2O$ (1636 $cm^{-1}$) disappeared in 50% O-LS, suggesting that $H_2O$ content reduced with the replacement of the hydrated cations with surfactant cation ions. This implies that the surface properties of Na-LS changed from hydrophilic to hydrophobic with the presence of the surfactant. These observations are highly similar to those reported by Wang and Wang.[17]

### Structure of Corn Starches

Figure 5 shows the FTIR spectrum of native and 15% modified starches in which the peak wave number with 1149 $cm^{-1}$ was ascribed to the C—O bond stretching of the —C—O—H group in starch. The characteristic peaks at 1014 and 1070 $cm^{-1}$ were attributed to C—O bond stretching of the —C—O—C group in the anhydroglucose ring of starch.[18–20] Bands observed for 15% modified starch between 1050–990 and 1350–1250 $cm^{-1}$ were assigned to the P—O—C and P═O stretching, respectively.[21–24] At the same time, an increase was observed between the bands of 1150–1014 $cm^{-1}$ for 15% modified starch compared with native starch. In addition to these peaks, the peak at 2350 $cm^{-1}$ observed for modified starch was assigned to P—OH group resulting from the crosslinking. The peak at 1637 $cm^{-1}$ is the characteristic peak and presumably originates from tightly bound water present in the starch granule.[18,20,25]

The broad band at 2110–2060 $cm^{-1}$ is the combination band arising from water alone.[26] An extremely broad band resulting

**Table III.** Gelatinization Temperature and Gelatinization Enthalpy of Native and 15% Modified Starches

| Starch type | $T_o$ (°C) | $T_p$ (°C) | $T_c$ (°C) | $\Delta H$ (J $g^{-1}$) |
|---|---|---|---|---|
| Native | 58.98 | 63.74 | 71.14 | 2.322 |
| 15% Modified | 56.56 | 60.87 | 67.87 | 1.750 |

$T_o$, onset temperature; $T_p$, peak temperature; $T_c$, completion temperature; $\Delta H$, gelatinization enthalpy.

**Table IV.** Physical Stability and Mechanical Integrity of the Produced Biocomposite Films After 1 Month at Room Condition

| Composite film formulation based on coded levels | | | | | |
|---|---|---|---|---|---|
| A | B | C | D | Stability | Integrity |
| N | 54/46 | 0.70 | 50% O-LS | Poor | Brittle |
| 10M | 54/46 | 0.45 | 15% O-LS | Poor | Brittle |
| 15M | 54/46 | 0.25 | Na-LS | Good | Flexible |
| 15M | 60/40 | 0.70 | 25% O-LS | Poor | Brittle |
| 15M | 63/37 | 0.45 | 50% O-LS | Poor | Brittle |

from vibration of the hydroxyl groups (O—H), which appeared at 3000 and 3700 $cm^{-1}$ at the same time, is the characteristic peak for starch.[18,20,27] The intensity of this peak for 15% modified starch is larger than that for native starch, indicating that the 15% modified starch with hydroxypropyl groups is hydrophilic compared with the native starch.

These observations explain how good compatibility at the interface between 15% modified starch and unmodified LS was achieved. Starch modification by hydroxypropylation helps starch form films with a high hydrophilic nature relative to native starch. On the other hand, HTAC modification makes LS more hydrophobic than Na-LS by cationic exchange. Thus, 15% modified starch exhibiting a higher hydrophilicity than native starch can be more compatible with Na-LS exhibiting a higher hydrophilicity than 50% O-LS. Furthermore, the compatibility between 15% modified starch and Na-LS makes their biodegradable composite film flexible, as they absorb moisture from the surrounding air at room conditions owing to their hydrophilic nature.

Table III gives gelatinization temperature and gelatinization enthalpy of native and 15% modified starches. In this table, it was interpreted that $T_o$, $T_p$, and $T_c$ values of 15% modified starch are lower than those of the native starch. This means that it requires low degree of heating energy than the native starch. Gelatinization enthalpy reflects the energy required to disrupt the starch granule structure.[28,29] Hydroxypropyl groups are hydrophilic in nature. When introduced into the starch granule, they weaken and strain the internal bond structure holding the granule together.[30,31] In addition to this, the decrease in $\Delta H$ on hydroxypropylation suggests that hydroxypropyl groups disrupt double helices resulting from the rotation of the flexible hydroxypropyl groups within the amorphous regions of the granule.[32] Controversially, crosslinking reinforces the granule of starch and prevents gelatinization, so more heat is needed for the sake of gelatinization.[28,29,32] The preparation procedure for dual-modified starch affects the product properties. Crosslinking reduces the degree of subsequent hydroxypropylation, and hydroxypropylation increases the degree of subsequent crosslinking.[28]

In this study, crosslinking degree remains intact, whereas hydroxypropylation degree was increased by a factor of 5%. It is for this reason that hyroxypropylation prevails against the crosslinking. In addition to this, the hydroxypropyl groups assist 15% modified starch with forming films containing LSs more easily than the native starch, regardless of type or chemical modification of the LSs.

TGA thermograms of native starch and 15% modified starch were highly similar to each other, exhibiting a single-step decomposition line at about 280°C. The maximum weight losses for native and 15% modified starches were at about 337 (75.43%) and 334°C (81.45%), respectively. These findings show consistency with the findings reported by Aziz et al.[28] Based on the results obtained, it was determined that 15% modified starch slightly weakened thermal stability of native starch. This result is proportional to the results obtained by DSC, indicating that hydroxypropyl groups, when introduced to the starch granules, do absolutely weaken the internal bond structure holding the granule together, as presumably accepted.

### Structure of Biocomposite Film

Based on the Taguchi predictions, it was determined that LS addition is necessary for the sake of film strength, as the neat films ended up with a shape distortion and lost their structural integrity. With this respect, among 16 different types of the prepared biocomposite films, five survival biocomposite films, as explained earlier, were selected and stored at room temperature for 1 month to see the maintained stability. The most promising biocomposite film based on the observation of the texture

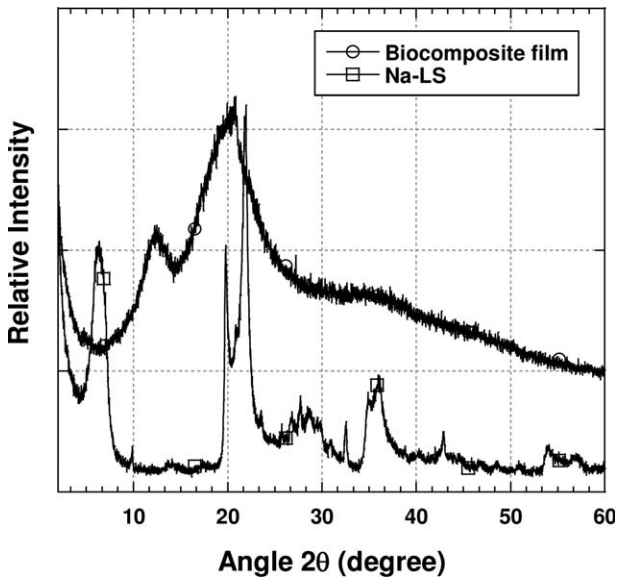


**Figure 6.** XRD patterns of biocomposite film and Na-LS.

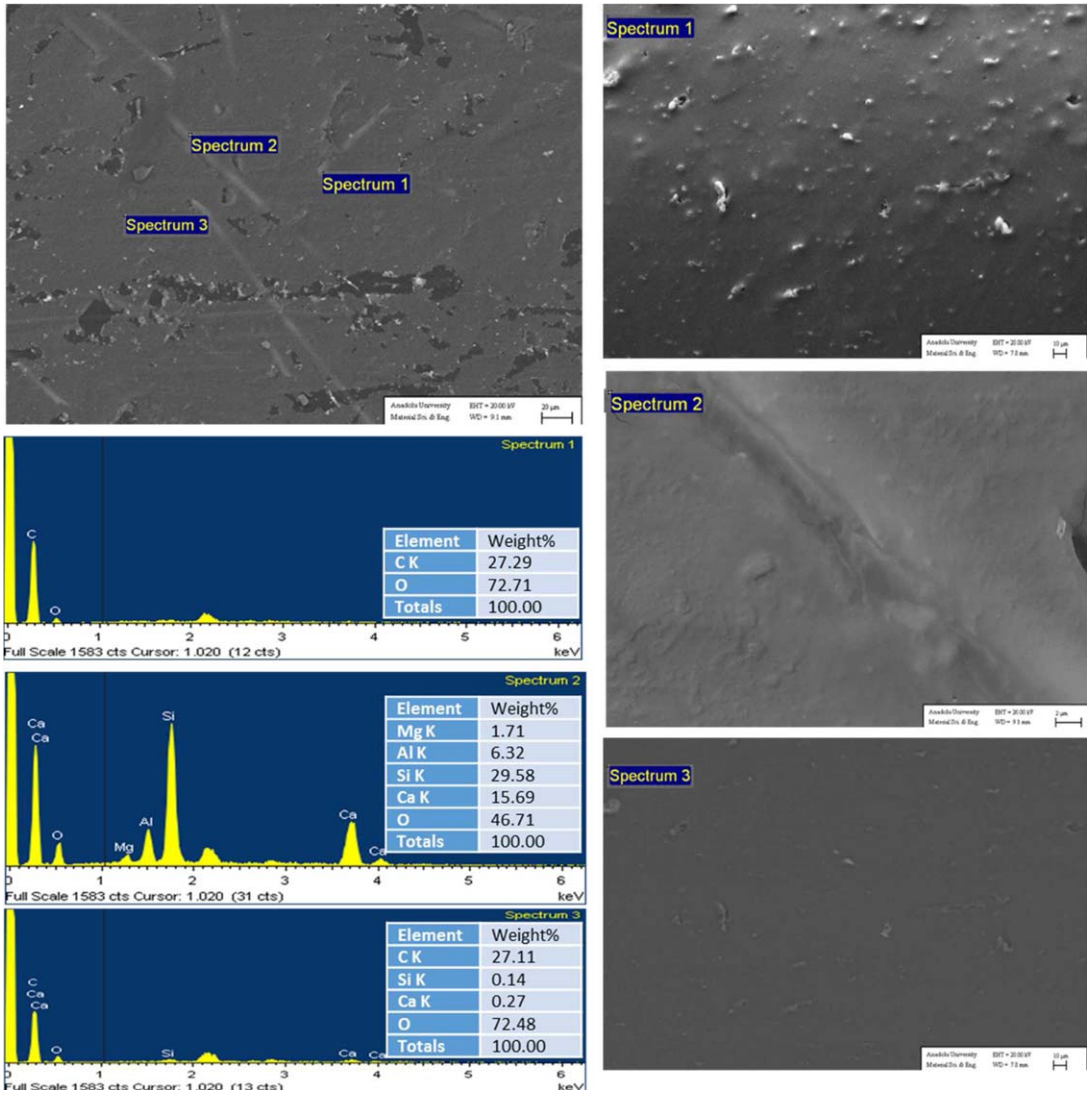


**Figure 7.** Fracture surface SEM image of biocomposite film and EDX spectra and elemental composition of the biocomposite film from the different areas. [Color figure can be viewed in the online issue, which is available at wileyonlinelibrary.com.]

structure and mechanical integrity was then concluded. Table IV gives the resulting texture structure and mechanical integrity of the five survival biocomposite films following 1 month at room condition. All the films, except for the one based on 54/46 pectin jelly/starch ratio of 15% modified starch and 0.25% of Na-LS, seemed to be brittle after observed for 1 month at room condition. This implies that even if the composite films are initially elastic, storage conditions as well as compatibility between the types of starch and the LS, or in other words, their interfacial interactions play a pivotal role in shaping out their final properties. This is why pectin jelly/15% modified starch-based biocomposite films (54/46 w/w) containing 0.25 wt % of Na-LS emerge as the most promising in terms of packaging texture structure and mechanical integrity. Please be advised that the following characterization tests were carried out just only on that film.

In the literature, molecular weights of the amylose and amylopectin components of high amylose corn starch have been determined to be 1.5–2.8 $\times$ $10^5$ and 1.7 $\times$ $10^8$, respectively.[33] Shi et al.[34] calculated the $M_w$ of the thermoplastic starch as $(1.48 \pm 0.19) \times 10^6$ g mol$^{-1}$ using a static laser light scattering. In light of the discussion made in these studies, intrinsic viscosity and molecular weight of the most promising biocomposite film were calculated as 0.1973 dL g$^{-1}$ and 46590.64 g mol$^{-1}$, respectively, by using Mark–Houwink constants ($K = 13.2 \times 10^{-3}$ mL g$^{-1}$ and $a = 0.68$) given by Zeng et al.[35] The most promising biocomposite film with these properties seems to fulfill the requirements for being a packaging material with the needed texture structure and mechanical integrity. This is already indicated by a long-term exposure (1 month) at room temperature.

Figure 6 shows the XRD patterns for the biocomposite film and pristine Na-LS. As seen in this figure, biocomposite films were found not to exhibit any remarkable sign of peak apparent at $2\theta$ value of 6.16°, which corresponds to (001) Bragg reflection of Na-LS. Biocomposite film gives the peaks at $2\theta$ values of

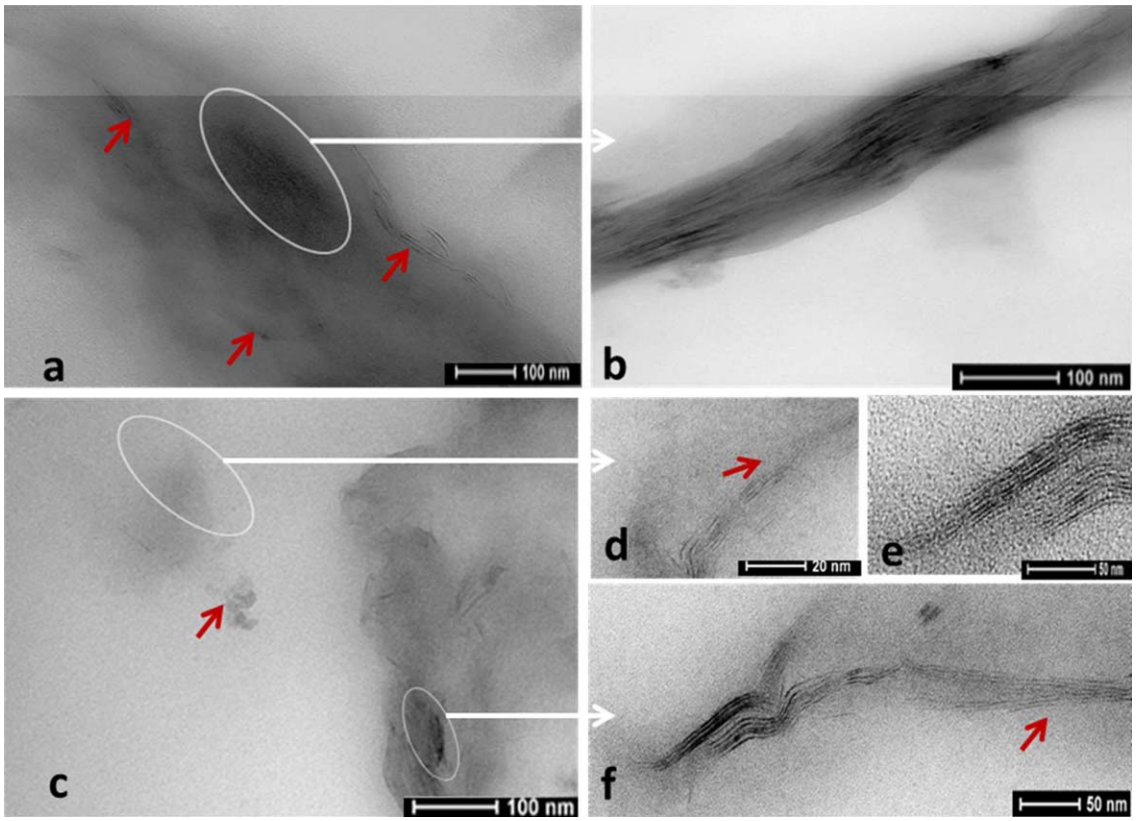


**Figure 8.** TEM images of the biocomposite film. [Color figure can be viewed in the online issue, which is available at wileyonlinelibrary.com.]

12.24° and 19.92°. These peaks are characteristic crystalline peaks for thermoplastic starch.[4]

This indicated that proper dispersion of Na-LS within biocomposite film was successfully accomplished. On the other hand, the nonexistence of the characteristic peak of Na-LS at around $2\theta$ values of 6.16° in XRD patterns may be resulting from very low content of Na-LS (0.25%) within biocomposite film matrix. In this case, the results obtained do not necessarily imply that Na-LSs were dispersed within biocomposite films individually and homogenously. Therefore, by SEM and EDX analyses, we search for further ample evidences to shed light on dispersion state of Na-LS within biocomposite film. In addition to this, a TEM investigation was performed to find out in what manner (exfoliated, intercalated, or combination of them) as well as to what extent the silicates were homogenously dispersed in biocomposite films.

Figure 7 shows the SEM images showing the fracture surface of the biocomposite film on the left side with the EDX findings underneath, as well as the selected regions at higher magnifications on the right side furnished with the corresponding spectrum prediction. EDX-aided SEM analysis was performed on the vertical structures in the different parts of the biocomposite film fracture surface. EDX spectra and elemental compositions were obtained from three different areas sectioned from biocomposite film fracture surface (homogenous, semihomogeneous, and heterogeneous). In brief, six elements were detected: C, O, Al, Si, Mg, and Ca. The carbon (C) was observed in the EDX because of the organic structure of the biocomposite film. The other elements constitute the elements most likely found in LSs. The weight percentages of these elements are too low to compare C and O ratio because of the very low content of the Na-LS (0.25%) in the biocomposite film matrix. Generally speaking, an ordered and parallel arrangement of vertical structures is preserved. Morphology is based on partly homogenously separated silicates accompanied by a few tiny agglomerates of silicates, as depicted in the SEM image called Spectrum 1. SEM image called Spectrum 2 proves that an ordered and parallel arrangement of vertical structure can be reasonably ascribed to intercalated LS structures based on the EDX analysis. Although it depends on the region of choice, the overall dispersion state of silicates seems good enough to maintain the texture structure and mechanical integrity, as expected in light of the previous promising results. When combined with morphological investigation performed by XRD findings, SEM–EDX examination findings are consistent with our approach that Na-LSs exhibit a preferential distribution within biocomposite film. To back up our approach by gaining a better insight into the morphological nature, TEM analysis was performed. Figure 8(a–f) depicts the TEM images. As seen in Figure 8(a,b), intercalated silicates appear to be around the locations indicated by the red arrows. In Figure 8(c), intercalated zones surrounded with little exfoliated zones are visible within the white-colored

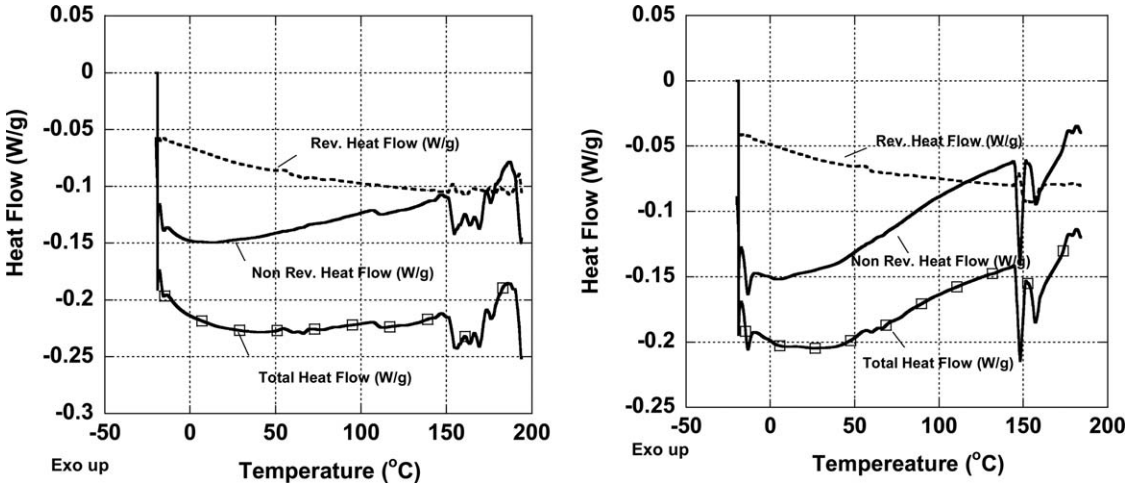


**Figure 9.** Modulated DSC thermogram for the biocomposite film (a) with LS and (b) without LS.

circles. A tiny agglomerated location is indicated by a red arrow in the same image. In Figure 8(d–f), the same locations of choice were examined at higher magnifications, which prove our approach that the main dispersion type of silicates within starch is intercalation.

Figure 9(a,b) shows the modulated DSC thermogram for the most promising biocomposite films with and without LS, respectively. Modulated temperature DSC is a promising method to measure the thermal behavior of materials. In this method, the response of the sample to a time-dependent signal (sinusoidal temperature change) is measured. $T_o$ properly evaluates thermal response of a material, and the measured data are separated into reversing and nonreversing components of heat flow. In other words, it erases the necessity of heat-cool-heat cycle procedure, improving the accuracy while saving some time for data sort-out and interpretation. As seen in Figure 9(a), biocomposite film exhibits two different glass transition zones in reversible side, one apparent around 57°C, whereas the other appears at around 150–160°C. When determining the glass transition temperature of starch-based thermoplastics using DSC, generally two different, so-called lower or higher $T_g$ values are separately or simultaneously found in the mixtures depending on the glycerol content in the solution mixture. This behavior is likely to be connected with the formation of a starch-rich area and glycerol-rich area that causes a partial phase separation. The higher and lower transitions seem to be characteristics for starch plasticized with glycerol and are independent of the processing method applied. In our case, this behavior may also be attributed to the presence of pectin jelly in the mixture together with glycerol. In this perspective, the lower $T_g$ may refer to $T_g$ of pectin jelly and glycerol-rich zone, whereas the higher $T_g$ may refer to starch-rich zone. This finding is consistent with the previous findings obtained. To see the effect of LS on the biocomposite film, an additional modulated DSC analysis was performed for the biocomposite film without LS [Figure 9(b)]. The effect of clay on the $T_g$ values for biocomposite film is insignificant. The same value of 57 was achieved once again. As seen in the nonreversible side, the effect of clay addition on crystallization seems to be significant. McGlashan and Peter [36] reported that the more intercalated LS in polymers, the more number of sites for crystal nucleation become active. Therefore, the crystallization rate and geometry of crystal growth are enhanced, as the gap between the layers increases. This is proportional to our findings as well. On the other hand, when looking at the melting enthalpy values, the enthalpy value is higher for the film with LS than the film without LS. This suggests that LSs act like a heat sink within biocomposite film.

Figure 10 shows the creep recovery of the most promising biocomposite and LDPE films, separately. After putting the experimentally determined values in the equation given earlier in experimental subsection, $J_{er}$ values were calculated to be $3.71 \times 10^{-9}$ and $4.81 \times 10^{-9}$ $m^2$ $N^{-1}$ for biocomposite and LDPE films, respectively. As the creep elasticity corresponds to $1/J_{er}$ value, it can be concluded that the biocomposite film is competitive and good in terms of elastic recovery ability compared with the corresponding LDPE film.

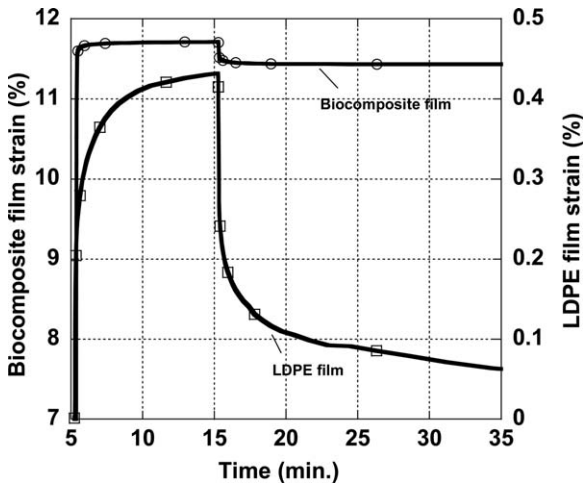


**Figure 10.** Creep recovery of biocomposite and LDPE film.

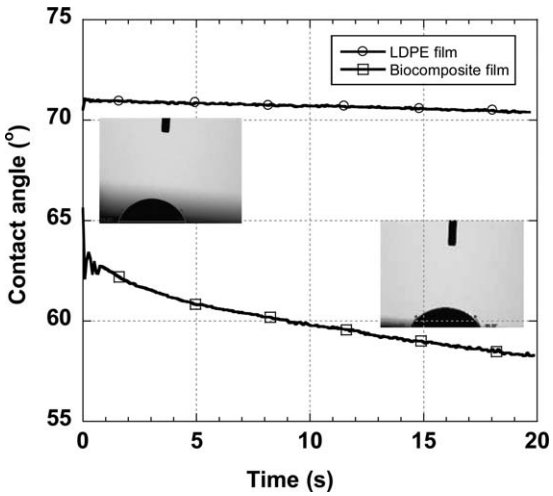


**Figure 11.** Contact angles of the biocomposite and LDPE film surfaces.

Figure 11 depicts the contact angle value of each surface. Water surface tension was found to be 72.16 mN $m^{-1}$. The average contact angle of the LDPE and biocomposite films was found to be $70.70° \pm 0.84°$ and $60.05° \pm 2°$, respectively. The result obtained reveals that LDPE film has higher hydrophobicity than biocomposite film. The information obtained from contact angle measurements holds the clue to the barrier properties of the both films used in this study. However, they need to be evaluated together with the measured values for the sake of performance comparison.

Important function for food packaging materials is to delay the water vapor transport into or out of the food. To select a packaging material for a food product, it is important to know the range in water activity ($a_w$) or moisture content that is necessary to preserve the food quality.[37] Based on the calculation procedure in the experimental part, WVTR (g $m^{-2}$ $h^{-1}$) was determined to be 9.87 and 8.59 g $m^{-2}$ $h^{-1}$, respectively, for biocomposite and LDPE films. We cannot judge whether the results obtained are good or bad, as it depends on the application area where the films are used. For example, to keep the activity of microorganisms to a minimum in dry foods, it is important to minimize the inflow of water, whereas fresh vegetables lose their texture if water activity is too low. On the other hand, fresh vegetables are usually picked before they ripen fully. During storage, they are therefore in need of oxygen to respire. A packaging material with moderate oxygen permeability is suitable here. Vegetable and animal fats react with oxygen in the presence of light. Aldehydes that formed make the fat rancid, leading to bad taste and flavor. This is especially critical for moist oil. These substances require a high-oxygen and light-barrier packaging material. The fat in both fresh and cured meat is susceptible to oxidation in the presence of air. It is, however, not a good solution in the short term to avoid oxygen, as anaerobic microbes may then grow on the fresh meat. $O_2$GTR of the biocomposite and LDPE films was determined to be $1366 \pm 194$ and $1838 \pm 125$ mL $m^{-2}$ $day^{-1}$, respectively. Theoretically speaking, the lower the $O_2$GTR, the better the packaging performance the film exhibits. So, from this point of view, we can conclude that the corresponding biocomposite film is better than the LDPE film in many cases in light of the discussion made above.

## CONCLUSIONS

In this study, orange peel-derived pectin jelly/corn starch-based biocomposite films with and without LSs were produced via melt extrusion followed by film die casting. To enhance the interfacial interactions, corn starch and LSs were chemically modified. Taguchi experimental analysis was executed to find the optimized combination of predictions for starch and LSs with and without chemical modifications. XRD, FTIR, DSC, TGA, and SEM were systematically used to characterize corn starch, LSs, and biocomposite film. It was determined that LS addition is necessary for composite film strength and flexibility. The 50% HTAC modification of LS enlarged the gallery spacing of the layers most, thus enabling native starch granules to penetrate into the gallery spacing as easily as possible. On the other hand, regardless of type or modification of the LSs, 15% modification of starch via hydroxypropylation was found to result in rigid and flexible films compared with neat starch. As a result, of all the films tested, pectin jelly/15% modified starch-based biodegradable composite films (54/46 w/w) containing 0.25 wt % of Na-LS emerged as the most promising in terms of texture structure and mechanical integrity. Intrinsic viscosity, molecular weight, XRD, SEM–EDX, and TEM analyses were performed to characterize the biocomposite film. Intrinsic viscosity and molecular weight showed the stability of the biocomposite film. In addition to this, XRD, SEM–EDX, and TEM indicated that Na-LSs exhibit a preferential distribution within biocomposite film. Creep recovery, hydrophobicity, WVTR, and $O_2$GTR of the most promising biocomposite films were measured and its overall packaging performance was evaluated and weighed against the performance of LDPE film. The analysis results showed that biocomposite film has remarkable specifications in terms of elasticity and barrier properties when compared with LDPE film, and that biocomposite films are capable to be safely used in some food packaging applications.

## ACKNOWLEDGMENTS

This study was supported by the Anadolu University Scientific Research Projects Commission under the grant no 1003F106. The authors thank Alp Özdemir, Oya Durukan, Ayşegül Tuna, Yiğitalp Okumuş, Assist. Prof. Dr. Göktuğ Günkaya, Assist. Prof. Dr. Hande Çelebi, and Prof. Dr. Rıdvan Say for their valuable contributions.

## REFERENCES

1. Cokaygil, Z. Biodegradable nanocomposite film production from orange peels and utilization as food packaging. PhD Thesis, Graduate School of Sciences, Anadolu University, Turkey, **2013**.
2. Mangiacapra, P.; Gorrasi, G.; Sorrentino, A.; Vittoria, V. *Carbohydr. Polym.* **2006**, *64*, 516.
3. Fishman, M. L.; Coffin, D. R. *Carbohydr. Polym.* **1998**, *35*, 195.

4. Yurdakul, H.; Durukan, O.; Seyhan, A. T.; Celebi, H.; Oksuzoglu, M.; Turan, S. *J. Appl. Polym. Sci.* **2013**, *127*, 812.
5. Aloisi, G. G.; Elisei, F.; Nocchetti, M.; Camino, G.; Frache, A.; Costantino, U.; Latterini, L. *Mater. Chem. Phys.* **2010**, *123*, 372.
6. Park, H. M.; Li, X. C.; Jin, C. Z.; Park, C. Y.; Cho, W. J.; Ha, C. S. *Macromol. Mater. Eng.* **2002**, *287*, 553.
7. Ray, S. S.; Bousmina, M. *Prog. Mater. Sci.* **2005**, *50*, 962.
8. Majdzadeh-Ardakani, K.; Navarchian, A. H.; Sadeghi, F. *Carbohydr. Polym.* **2010**, *79*, 547.
9. Coffin, D. R.; Fishman, M. L. *J. Agric. Food Chem.* **1993**, *41*, 1192.
10. Coffin, D. R.; Fishman, M. L. *J. Appl. Polym. Sci.* **1994**, *54*, 1311.
11. Fishman, M. L.; Coffin, D. R.; Onwulata, C. I.; Konstance, R. P. *Carbohydr. Polym.* **2004**, *57*, 401.
12. Cho, C. W.; Lee, D. Y.; Kim, C. W. *Carbohydr. Polym.* **2003**, *54*, 21.
13. Erdogan, B. C.; Seyhan, A. T.; Ocak, Y.; Tanoglu, M.; Balkose, D.; Ulku, S. *J. Therm. Anal. Calorim.* **2008**, *94*, 743.
14. Ranganna, S. In Handbook of Analysis and Quality Control for Fruit and Vegetable Products; Tata Mc Graw Hill: New Delhi, **2008**; Chapter 2, p 42.
15. Tabtiang, A.; Lumlong, S.; Venables, R. A. *Eur. Polym. J.* **2000**, *36*, 2559.
16. Saka, G.; Diltemiz, S. E.; Ozcan, A. A.; Ersoz, A.; Say, R. *Hacettepe J. Biol. Chem.* **2008**, *36*, 207.
17. Wang, L.; Wang, A. Q. *J. Hazard. Mater.* **2008**, *160*, 173.
18. Ruan, H.; Chen, Q. H.; Fu, M. L.; Xu, Q.; He, G. Q. *Food Chem.* **2009**, *114*, 81.
19. Dai, H. G.; Chang, P. R.; Yu, J. G.; Geng, F. Y.; Ma, X. F. *Carbohydr. Polym.* **2010**, *80*, 139.
20. Chi, H.; Xu, K.; Xue, D. H.; Song, C. L.; Zhang, W. D.; Wang, P. X. *Food Res. Int.* **2007**, *40*, 232.
21. Coates, J. In Interpretation of Infrared Spectra, A Practical Approach; Meyers, R. A., Ed.; Wiley: Chichester, **2000**; p 10815.
22. Mi, F. L.; Sung, H. W.; Shyu, S. S.; Su, C. C.; Peng, C. K. *Polymer* **2003**, *44*, 6521.
23. Singh, A. V.; Nath, L. K. *Starch-Starke* **2011**, *63*, 655.
24. Murua-Pagola, B.; Beristain-Guevara, C. I.; Martinez-Bustos, F. *J. Food Eng.* **2009**, *91*, 380.
25. Zhang, S. D.; Zhang, Y. R.; Zhu, J.; Wang, X. L.; Yang, K. K.; Wang, Y. Z. *Starch-Starke* **2007**, *59*, 258.
26. Li, W.; Dobraszczky, B. J.; Dias, A.; Gil, A. M. *Cereal Chem.* **2006**, *83*, 407.
27. Junistia, L.; Sugih, A. K.; Manurung, R.; Picchioni, F.; Janssen, L. P. B. M.; Heeres, H. J. *Starch-Starke* **2008**, *60*, 667.
28. Aziz, A.; Daik, R.; Ghani, M. A.; Daud, N. I. N.; Yamin, B. M. *Malaysian J. Chem.* **2004**, *6*, 48.
29. Liu, H. J.; Ramsden, L.; Corke, H. *Starch-Starke* **1999**, *51*, 249.
30. Perera, C.; Hoover, R. *Food Chem.* **1999**, *64*, 361.
31. Perera, C.; Hoover, R.; Martin, A. M. *Food Res. Int.* **1997**, *30*, 235.
32. Morikawa, K.; Nishinari, K. *Carbohydr. Polym.* **2000**, *43*, 241.
33. Shogren, R. *Biomacromolecules* **2007**, *8*, 3641.
34. Shi, R.; Zhang, Z.; Liu, Q.; Han, Y.; Zhang, L.; Chen, D.; Tian, W. *Carbohydr. Polym.* **2007**, *69*, 748.
35. Zeng, W.; Du, Y.; Xue, Y.; Frisch, H. L. In Mark-Houwink-Staudinger-Sakurada Constants; Mark, J. E., Ed.; Springer Science: New York, **2007**; p 305.
36. McGlashan, S. A.; Peter, J. H. *Polym. Int.* **2003**, *52*, 1767.
37. Hedenqvist, M. S. In Barrier Packaging Materials; Kutz, M., Ed; Myer Kutz Associates Inc.: New York, **2005**; p 547.